Int. J. Electrochem. Sci., 17 **(2022)** Article Number: 220548, doi: 10.20964/2022.05.43

International Journal of
ELECTROCHEMICAL
SCIENCE
www.electrochemsci.org

Short Communication

Preparation of Zinc-manganese Phosphating Coating on Q235 Steel and Its Environmental-friendly Sealing Treatment

Xiaohua Yu[1,2,*], *Ruwei Wang*[2], *Laishun Yang*[1]

[1] College of Civil Engineering and Architecture, Shandong University of Science and Technology, Qingdao 266590, China
[2] Qingdao Intrgrity Environmental Protection Science and Technology Co., Ltd, Qingdao 266109, China
[*]E-mail: Yu_edu590@126.com

Received: 6 February 2022 / *Accepted:* 12 March 2022 / *Published:* 5 April 2022

Zinc-manganese phosphating coating was prepared on the surface of Q235 steel, followed by post-treatment via different environmental-friendly sealing processes, such as oil immersion sealing process, silicate sealing process and rare earth salt sealing process. The surface morphology, phase composition, thickness, surface wettability and corrosion resistance of zinc-manganese phosphating coating were tested and analyzed. The results show that the surface of Q235 steel is completely covered with zinc-manganese phosphating coating composed of $Zn_3(PO_4)_2 \cdot 4H_2O$, $Mn_2Zn(PO_4)_2 \cdot 4H_2O$ and $Zn_2Fe(PO_4)_2 \cdot 4H_2O$ phases, which can inhibit the corrosion process of Q235 steel. After post-treatment via different environmental-friendly sealing processes, the surface roughness of zinc-manganese phosphating coating is reduced and the corrosion resistance is further improved, but its thickness and phase composition changes are small. The compactness of zinc-manganese phosphating coating after rare earth salt sealing treatment is the best, showing good hydrophobicity and better corrosion resistance for Q235 steel.

Keywords: Zinc-manganese phosphating coating; Q235 steel; Environmental-friendly sealing treatment; Corrosion resistance

1. INTRODUCTION

Phosphating is an important surface treatment for steel surface protection. As a non-conductive and insoluble coating, phosphating coating can inhibit the formation of microcells on steel surface, so as to effectively slow down corrosion [1-5]. According to different coating-forming systems, phosphating coatings were mainly divided into iron phosphating coating, zinc phosphating coating, zinc-calcium phosphating coating, zinc-manganese phosphating coating and manganese phosphating coating [6-10]. No matter what kind of phosphating coating, there are some cracks and holes on its

surface. These defects will reduce the compactness of phosphating coating, and gradually become a channel for the corrosion medium to penetrate into the interface between the phosphating coating and the substrate, resulting in the decrease of corrosion resistance.

Therefore, it is necessary to take measures to seal the surface of phosphating coating, which will effectively improve the corrosion resistance of phosphating coating while also filling the defects. The chromate sealing process is usually used in the industry, although this process has a good sealing effect, it will gradually be replaced by an environmental-friendly sealing process due to its high toxicity and great harm to the environment [11-12]. The silicate sealing process and rare earth salt sealing process have been proved can be used for phosphating coating sealing treatment, and it is expected to become an ideal environmental-friendly sealing process to replace chromate sealing process [13-15]. At present, there are some reports on the separate studies of silicate sealing process and rare earth salt sealing process, but there are few reports on the sealing treatment of phosphating coating using different environmental-friendly sealing processes and comparing the advantages and disadvantages of sealing effect.

In this paper, zinc-manganese phosphating coating was prepared on the surface of Q235 steel, followed by post-treatment via different environmental-friendly sealing processes, such as oil immersion sealing process, silicate sealing process and rare earth salt sealing process. By examining the surface morphology, phase composition, and corrosion resistance of the phosphating coating after sealing treatment, researchers hope to develop a more environmental-friendly sealing process that will effectively improve the corrosion resistance of zinc-manganese phosphating coating while reducing harm to meet environmental requirements.

2. EXPERIMENTAL

2.1 Materials and pre-treatment

Q235 steel sheet of 24 mm×12 mm×1.5 mm was used as the experimental material. The pre-treatment process before phosphating process was as follows: different kinds of sandpaper polishing (800#~2000# sandpaper) → alkali solution degrease (sodium carbonate 45 g/L, sodium hydroxide 12 g/L, 65℃ for 8 min) → dilute hydrochloric acid activation (volume fraction 10%, room temperature for 1 min) → cleaning (distilled water at room temperature) → drying (cold air drying).

2.2 Preparation of zinc-manganese phosphating coating

The zinc dihydrogen phosphating, zinc nitrate, manganese nitrate, sodium fluoride and citric acid (analytical reagent) were used to prepare zinc-manganese phosphating solution. The technology parameters and solution composition are as follows: zinc dihydrogen phosphating 40 g/L, zinc nitrate 60 g/L, manganese nitrate 20 g/L, sodium fluoride 1 g/L, citric acid 1.5 g/L. The temperature of phosphating solution was maintained at (65±0.5)℃. The treated Q235 steel sheet was immersed in phosphating solution by suspension method for 20 minutes to prepare zinc-manganese phosphating

coating.

2.3 Environmental-friendly sealing treatment

Zinc-manganese phosphating coating was post-treatment via oil immersion sealing process, silicate sealing process and rare earth salt sealing process respectively. The solution composition and technology conditions used in each process are shown in Table 1. Environmental-friendly reagents are used to prepare the solutions, which reduce the degree of pollution and harm. For ease of expression, the zinc-manganese phosphating coatings sealed by oil immersion sealing process, silicate sealing process and rare earth salt sealing process will be respectively referred to as oil sealed zinc-manganese phosphating coating, silicate sealed zinc-manganese phosphating coating and rare earth sealed zinc-manganese phosphating coating.

Table 1. Solution composition and technology conditions of different environmental-friendly sealing processes

Different environmental-friendly sealing processes	**Solution composition**	**Technology parameters**
oil sealing	commercially available anti-rust oil	room temperature, 6 min
silicate sealing	sodium silicate 20 g/L, thiourea 2 g/L, surfactant 1~1.5 g/L	80℃, 12 min
rare earth sealing	cerium nitrate 20 g/L, hydrogen peroxide 26 mL/L	45℃, 5 min

2.4 Characterization and properties testing

2.4.1 Surface morphology and phase composition

MERLIN Compact scanning electron microscope was used to characterize the surface morphology of different zinc-manganese phosphating coatings, and X'Pert pro X-ray diffractometer was used to characterize the phase composition of different zinc-manganese phosphating coatings. The voltage was 40 kV, the current was 30 mA, the scan rate was 4°/min, and the scan angle was ranged from 20° to 90°. X-max80 energy dispersive spectrometer was used to analyze the surface component of different zinc-manganese phosphating coatings. The surface scanning mode was set to obtain the distribution of each element in the zinc-manganese phosphating coating.

2.4.2 Thickness measurement

TT260 thickness gauge was used to measure the thickness of different zinc-manganese phosphating coatings. In order to reduce the measurement error, five points were randomly selected on

the surface of zinc-manganese phosphating coating, and the measurement results were averaged.

2.4.3 Surface wettability testing

DSA100 contact angle measuring instrument was used to measure the contact angle of water droplet, which was used to evaluate the surface wettability of different zinc-manganese phosphating coatings. The water droplet with volume of 4 μL was placed at three different positions on the surface of zinc-manganese phosphating coating, and the measured contact angles were averaged to reduce the error.

2.4.4 Corrosion resistance testing

The VSP-300 electrochemical workstation was used to simulate electrochemical corrosion, and the potentiodynamic polarization curve and electrochemical impedance spectroscopy of different zinc-manganese phosphating coatings were tested respectively. The corrosion medium is 3.5% sodium chloride solution with 1 mV/s scan rate. The auxiliary electrode is a platinum electrode while the working electrode is a zinc-manganese phosphating coating sample. A saturated calomel electrode is chosen as the reference electrode. The scan range of electrochemical impedance spectroscopy is 10^5~10^{-2} Hz and the amplitude of sine wave disturbance signal is 10 mV.

A mixed solution of copper sulfate, sodium chloride and diluted hydrochloric acid was prepared. The specific solution composition were: copper sulfate 41 g/L, sodium chloride 35 g/L, and 0.1 mol hydrochloric acid 13 mL/L. The anti-dripping performance of different zinc-manganese phosphating coatings was measured. Three drops of the solution were randomly dropped on the surface of zinc-manganese phosphating coating, and the time for the droplets to change color completely was recorded.

The corrosion resistance of different zinc-manganese phosphating coatings was evaluated based on the fitting results of potentiodynamic polarization curve and electrochemical impedance spectroscopy, as well as the anti-dripping performance.

3. RESULT AND DISCUSSION

3.1 Surface morphology and phase composition of different zinc-manganese phosphating coatings

Figure 1 shows the surface morphology of Q235 steel and different zinc-manganese phosphating coatings. Compared to Figure 1(a) and 1(b), it can be seen that zinc-manganese phosphating coating completely covers the surface of Q235 steel, showing a fault-like morphology with many rough local cracks and holes, which is a kind of typical morphology of phosphating coating [16-18]. Compared with unsealed zinc-manganese phosphating coating, the morphology of oil sealed zinc-manganese phosphating coating does not change significantly, and there were still more cracks and holes on the surface, as shown in Figure 1(c). The anti-rust oil is physically adsorbed on the

surface of zinc-manganese phosphating coating to form an oil coating, without chemical reaction.

As shown in Figure 1(d) and 1(e), the surface morphology of silicate sealed zinc-manganese phosphating coating and rare earth sealed zinc-manganese phosphating coating are different from that of oil sealed zinc-manganese phosphating coating. The cracks, holes and surface roughness of samples after sealing are reduced significantly. This is because silicate solution can dissolve the loose surface layer of zinc-manganese phosphating coating and the water-soluble residues of inclusion to play a role of leveling. In addition, silicate solution can also react with zinc-manganese phosphating coating. The reaction products deposited on the surface of zinc-manganese phosphating coating also play a role of filling defects, so as to improve its compactness. The reaction of zinc-manganese phosphating coating in rare earth salt solution is listed as Equation 1 to Equation 5 [19-20]. The formation of cerium oxide, cerium hydroxide and phosphating with different valence states can fill the defects on the surface of zinc-manganese phosphating coating, thus improving its compactness. In comparison, zinc-manganese phosphating coating produces more reaction products in rare earth salt solution and has a better effect of filling defects. Therefore, the surface of rare earth sealed zinc-manganese phosphating coating is compact with smaller roughness.

$$Ce^{3+} + 3OH^- \rightarrow Ce(OH)_3 \downarrow \quad (1)$$

$$Ce^{4+} + 4OH^- \rightarrow Ce(OH)_4 \downarrow \quad (2)$$

$$Ce^{4+} + 4OH^- \rightarrow Ce(OH)_4 \downarrow \quad (3)$$

$$Ce(OH)_4 \rightarrow CeO_2 + 2H_2O \quad (4)$$

$$Ce^{3+} + PO_4^{3-} \rightarrow CePO_4 \quad (5)$$

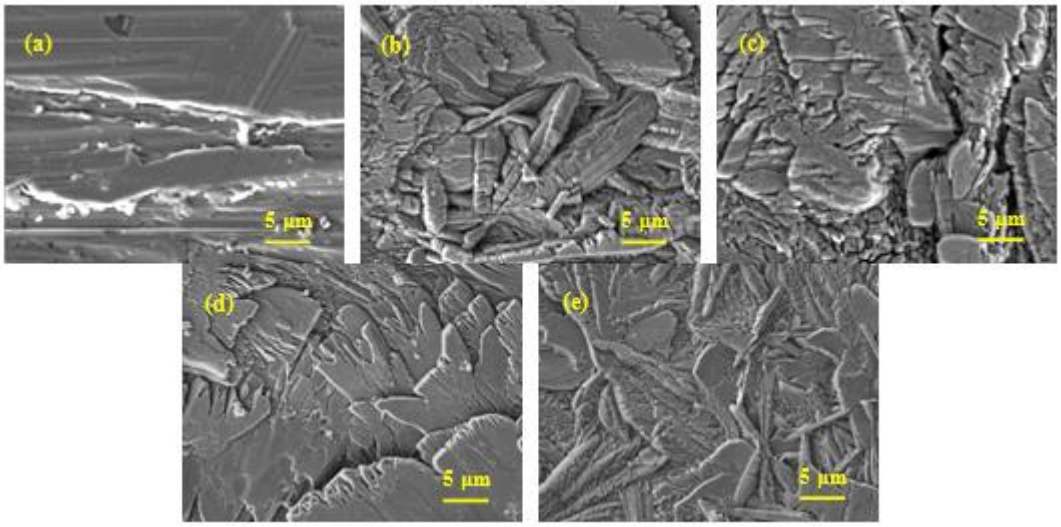

Figure 1. Surface morphology of Q235 steel and different zinc-manganese phosphating coatings; a-Q235 steel; b-unsealed zinc-manganese phosphating coating; c-oil sealed zinc-manganese phosphating coating; d-silicate sealed zinc-manganese phosphating coating; e-rare earth salt sealed zinc-manganese phosphating coating; (acceleration voltage is 10 kV, magnification is 2000 times)

Figure 2 shows the XRD patterns of different zinc-manganese phosphating coatings. The XRD

pattern analysis shows that the phase composition of untreated zinc-manganese phosphating coating are mainly $Zn_3(PO_4)_2 \cdot 4H_2O$, $Mn_2Zn(PO_4)_2 \cdot 4H_2O$ and $Zn_2Fe(PO_4)_2 \cdot 4H_2O$ which is almost the same as that of oil sealed zinc-manganese phosphating coating and rare earth sealed zinc-manganese phosphating coating. The similar structure of zinc-manganese phosphating coating and zinc compound is also reported [21-22]. However, the phase composition of silicate sealed zinc-manganese phosphating coating is different. In addition to $Zn_3(PO_4)_2 \cdot 4H_2O$, $Mn_2Zn(PO_4)_2 \cdot 4H_2O$ and $Zn_2Fe(PO_4)_2 \cdot 4H_2O$ phases, it also contains Na_2SiO_3 and $ZnSiO_3$ phases with small diffraction peaks. There is no phase related to the rare earth cerium element in rare earth sealed zinc-manganese phosphating coating. It may because that the content of rare earth cerium salt in zinc-manganese phosphating coating is less and mainly concentrated on the surface.

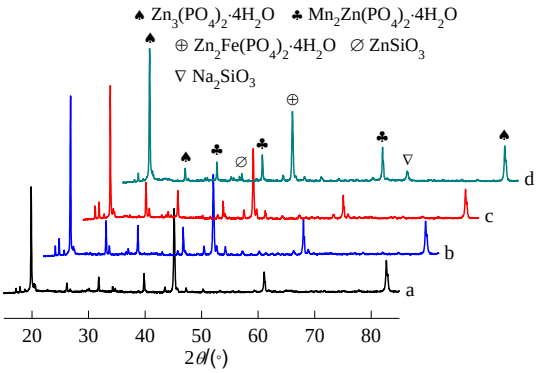

Figure 2. XRD patterns of different zinc-manganese phosphating coatings; a-unsealed zinc-manganese phosphating coating; b-oil sealed zinc-manganese phosphating coating; c-silicate sealed zinc-manganese phosphating coating; d-rare earth salt sealed zinc-manganese phosphating coating; (voltage is 40 kV and current is 30 mA, scan angle is ranged from 20° to 90° at the scan rate of 4°/min)

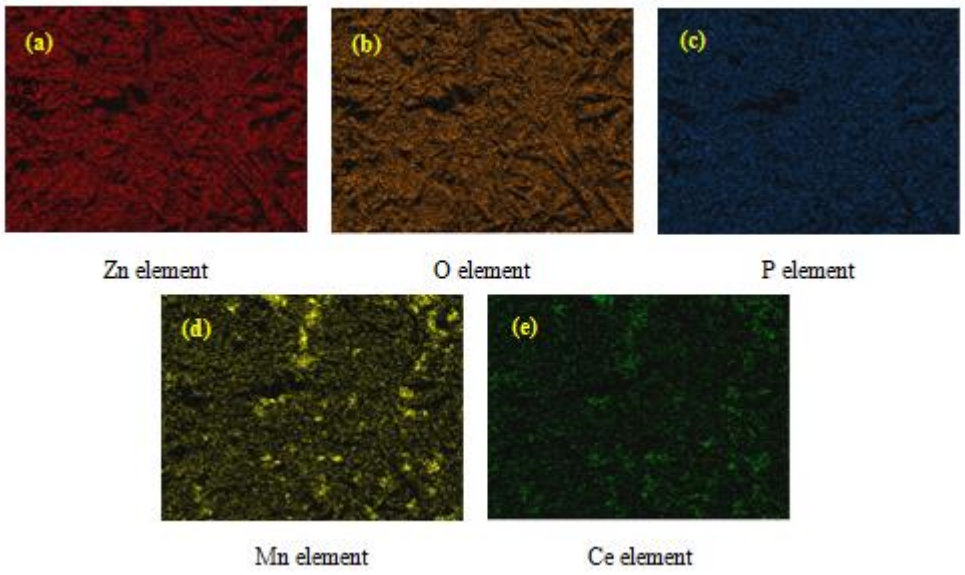

Figure 3. Distribution of elements on the surface of rare earth salt sealed zinc-manganese phosphating coating; (acceleration voltage is 5 kV with surface scanning mode and 1 μm sampling depth)

According to XRD pattern of rare earth sealed zinc-manganese phosphating coating, although the phase of rare earth element Ce is not found, rare earth element Ce is detected as the surface scan elements distribution shown in Figure 3. It is confirmed that the rare earth salt chemical reaction happens in the sealing process to generate compounds containing Ce.

3.2 Thickness and surface wettability of different zinc-manganese phosphating coatings

Figure 4 shows the thickness of different zinc-manganese phosphating coatings. It can be seen from Figure 4 that the thickness of oil sealed zinc-manganese phosphating coating, silicate sealed zinc-manganese phosphating coating and rare earth sealed zinc-manganese phosphating coating are basically the same as that of untreated zinc-manganese phosphating coating. This indicates that different sealing processes have little effect on the thickness of zinc-manganese phosphating coating, so the influence of different thickness on the corrosion resistance of zinc-manganese phosphating coating can be ignored.

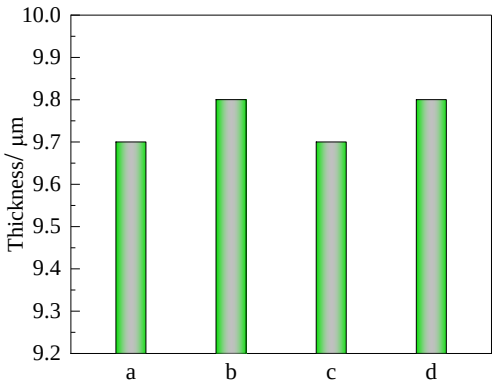

Figure 4. Thickness of different zinc-manganese phosphating coatings; a-unsealed zinc-manganese phosphating coating; b-oil sealed zinc-manganese phosphating coating; c-silicate sealed zinc-manganese phosphating coating; d-rare earth salt sealed zinc-manganese phosphating coating; (five randomly selected points were measured and averaged, the accuracy is 0.1 μm)

Figure 5 shows the droplet contact angle of Q235 steel and different zinc-manganese phosphating coatings. According to the analysis of droplet contact angle, the surface of Q235 steel, untreated zinc-manganese phosphating coating and oil sealed zinc-manganese phosphating coating are all hydrophilic, which leads to the easy spreading and larger contact area of corrosive medium. The surface of silicate sealed zinc-manganese phosphating coating and rare earth sealed zinc-manganese phosphating coating are both hydrophobic. The change of the surface of zinc-manganese phosphating coating from hydrophilic to hydrophobic hinders the spreading of the corrosive medium and reduces the contact area between the phosphating coating and corrosive medium, which is beneficial to improve the corrosion resistance. The relationship between hydrophobicity and corrosion resistance performance is studied in some papers [23-25].

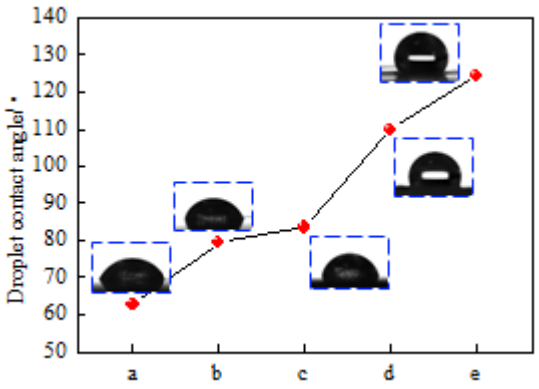

Figure 5. Droplet contact angle of Q235 steel and different zinc-manganese phosphating coatings; a-Q235 steel; b-unsealed zinc-manganese phosphating coating; c-oil sealed zinc-manganese phosphating coating; d-silicate sealed zinc-manganese phosphating coating; e-rare earth salt sealed zinc-manganese phosphating coating; (droplet volume is 4 μL and measurement accuracy is 0.1°)

3.3 Corrosion resistance of different zinc-manganese phosphating coating

3.3.1 Potentiodynamic polarization curve and electrochemical impedance spectroscopy analysis

Figure 6 shows the potentiodynamic polarization curves of Q235 steel and different zinc-manganese phosphating coatings, and Table 2 shows the electrochemical corrosion parameters related to the potentiodynamic polarization curve. Combined with Figure 6 and Table 2, it can be seen that the corrosion current density of unsealed zinc-manganese phosphating coating is significantly lower than that of Q235 steel, and the corrosion current density of zinc-manganese phosphating coating is further reduced after treatment by different environmental-friendly sealing processes. Among them, the corrosion current density of silicate sealed zinc-manganese phosphating coating and rare earth sealed zinc-manganese phosphating coating is relatively low, mainly because their surface roughness is reduced, and the corrosion resistance of corrosive ions is blocked to enhance ability to inhibit corrosion development. Materials with even and smaller roughness surface are beneficial to improve corrosion resistance performance [26-30]. In addition, their surfaces are both hydrophobic, which can further increase the corrosion resistance and inhibit the corrosion process.

Since rare earth sealed zinc-manganese phosphating coating has the best compactness and better surface hydrophobicity, the corrosion current density is the lowest and the corrosion resistance is relatively better.

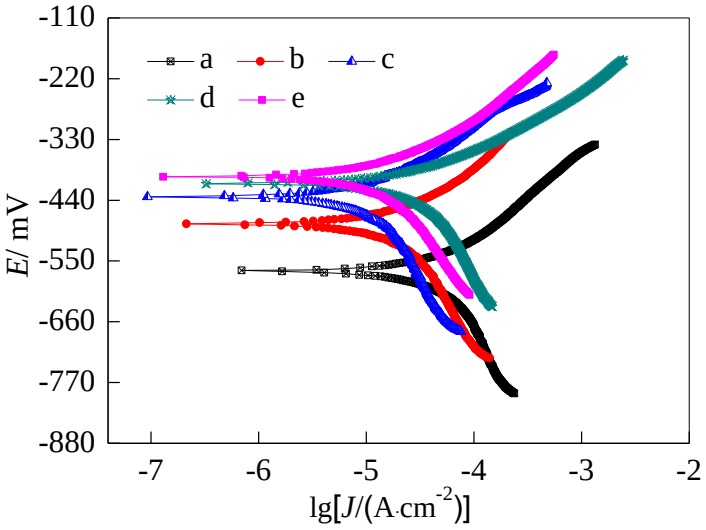

Figure 6. Potentiodynamic polarization curves of Q235 steel and different zinc-manganese phosphating coatings in 3.5% sodium chloride solution; a-Q235 steel; b-unsealed zinc-manganese phosphating coating; c-oil sealed zinc-manganese phosphating coating; d-silicate sealed zinc-manganese phosphating coating; e-rare earth salt sealed zinc-manganese phosphating coating; (auxiliary electrode is platinum electrode, working electrode is zinc-manganese phosphating coating sample and reference electrode is saturated calomel electrode, scan rate 1 mV/s)

Table 2. Electrochemical corrosion parameters related to potentiodynamic polarization curves

Different samples	**Corrosion potential/ mV**	**Corrosion current density/ (A·cm^{-2})**
Q235 steel	-568	1.0×10^{-4}
unsealed zinc-manganese phosphating coating	-485	3.1×10^{-5}
oil sealed zinc-manganese phosphating coating	-437	7.2×10^{-6}
silicate sealed zinc-manganese phosphating coating	-410	2.8×10^{-6}
rare earth salt sealed zinc-manganese phosphating coating	-396	1.6×10^{-6}

Figure 7 shows the electrochemical impedance spectroscopy of Q235 steel and different zinc-manganese phosphating coatings, and Table 3 shows the electrochemical corrosion parameters related to electrochemical impedance spectroscopy. Combined with Figure 7 and Table 3, it can be seen that the low-frequency impedance value of untreated zinc-manganese phosphating coating is increased by about 1.5 times compared with that of Q235 steel, and the maximum phase angle is increased from 48.3° to 53.4°. And the low-frequency impedance value and the maximum phase angle of zinc-manganese phosphating coating are further increased after post-treatment via different environmental-friendly sealing processes.

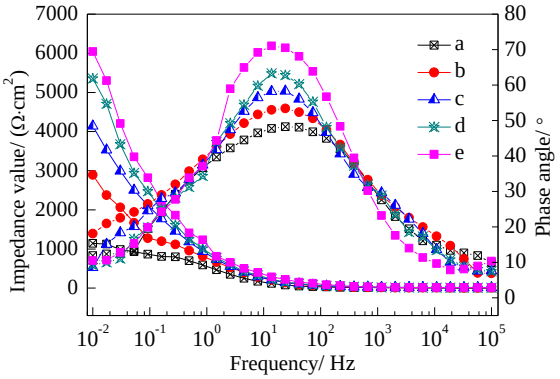

Figure 7. Electrochemical impedance spectroscopy of Q235 steel and different zinc-manganese phosphating coatings in 3.5% sodium chloride solution; a-Q235 steel; b-unsealed zinc-manganese phosphating coating; c-oil sealed zinc-manganese phosphating coating; d-silicate sealed zinc-manganese phosphating coating; e-rare earth salt sealed zinc-manganese phosphating coating; (auxiliary electrode is platinum electrode, working electrode is zinc-manganese phosphating coating sample and reference electrode is saturated calomel electrode, scan range of electrochemical impedance spectroscopy is 10^5~10^{-2} Hz and amplitude of sine wave disturbance signal is 10 mV)

The research shows that the increase of the low frequency impedance value and the maximum phase angle are the manifestations of the improved corrosion resistance of the coating. In comparison, the low-frequency impedance value and the maximum phase angle of silicate sealed zinc-manganese phosphating coating and rare earth sealed zinc-manganese phosphating coating are larger than that of oil sealed zinc-manganese phosphating coating, indicating better corrosion resistance which is consistent with the above potentiodynamic polarization curve analysis results.

Table 3. Electrochemical corrosion parameters related to electrochemical impedance spectroscopy

Different samples	**Low frequency impedance value/ (Ω·cm²)**	**Maximum phase angle/ °**
Q235 steel	1144.2	48.3
unsealed zinc-manganese phosphating coating	2893.8	53.4
oil sealed zinc-manganese phosphating coating	4139.7	58.3
silicate sealed zinc-manganese phosphating coating	5354.0	63.2
rare earth salt sealed zinc-manganese phosphating coating	6045.1	70.9

3.3.2 Anti-dripping performance

Figure 8 shows the anti-dripping performance of different zinc-manganese phosphating coatings. Generally speaking, the longer the anti-dripping time, the better the corrosion resistance of

the phosphating coating. On the contrary, the corrosion resistance of the phosphating coating is worse. The anti-dripping time of oil sealed zinc-manganese phosphating coating, silicate sealed zinc-manganese phosphating coating and rare earth sealed zinc-manganese phosphating coating is significantly longer than that of unsealed zinc-manganese phosphating coating. Sealing treatment enhances the ability of zinc-manganese phosphating coating to resist corrosive ion erosion. In particular, the rare earth salt sealed zinc-manganese phosphating coating has a anti-dripping time up to 210 s, which has better corrosion protection effect on Q235 steel. The effect of rare earth on corrosion resistance performance is investigated in some works [31-35].

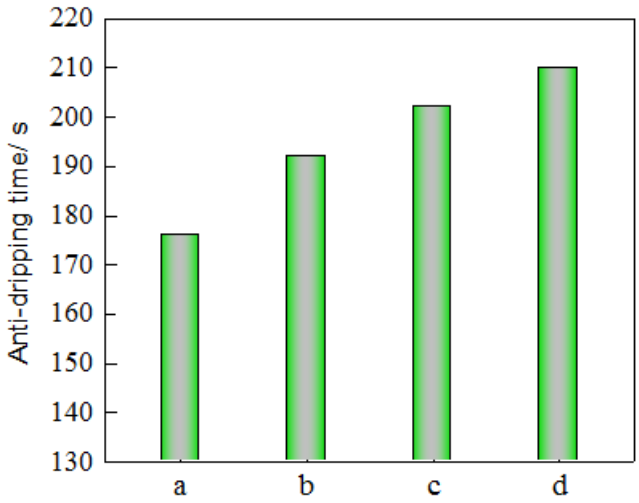

Figure 8. Anti-dripping performance of different zinc-manganese phosphating coatings; a-unsealed zinc-manganese phosphating coating; b-oil sealed zinc-manganese phosphating coating; c-silicate sealed zinc-manganese phosphating coating; d-rare earth salt sealed zinc-manganese phosphating coating; (dripping solution is composed of copper sulfate 41 g/L, sodium chloride 35 g/L and 0.1 mol hydrochloric acid 13 mL/L)

4. CONCLUSIONS

(1) A zinc-manganese phosphating coating composed of $Zn_3(PO_4)_2{\cdot}4H_2O$, $Mn_2Zn(PO_4)_2{\cdot}4H_2O$ and $Zn_2Fe(PO_4)_2{\cdot}4H_2O$ phases with a thickness of about 9.7 μm was prepared on the surface of Q235 steel, which can block corrosive ions and inhibit the corrosion process. After post-treatment via oil immersion sealing process, silicate sealing process and rare earth salt sealing process, the compactness of zinc-manganese phosphating coating was improved, and the corrosion resistance was further improved, but the thickness and phase composition changes were small.

(2) Compared with oil sealed zinc-manganese phosphating coating and silicate sealed zinc-manganese phosphating coating, rare earth sealed zinc-manganese phosphating coating has the best compactness, surface hydrophobicity and corrosion resistance, resulting in excellent corrosion protection effect on Q235 steel. The rare earth salt sealing process is the best environmental-friendly sealing process for zinc-manganese phosphating coating.

References

1. D. H. Xia, C. C. Pan, Z. B. Qin, B. M. Fan, S. Z. Song, W. X. Jin and W. B. Hu, *Prog. Org. Coat.*, 143 (2020) 105638.
2. S. Chimenti, J. M. Vega, E. Garcia-Lecina, H. J. Grande, M. Paulis, J. R. Leiza, *React. Funct. Polym.*, 143 (2019) 104334.
3. X. J. Cui, C. H. Liu, R. S. Yang, M. T. Li, X. Z. Lin and M. Gong, *Trans. Nonferrous Met. Soc. China*, 22 (2012) 2713.
4. H. B. Zhang and Y. Zuo, *Appl. Surf. Sci.*, 254 (2008) 4930.
5. X. J. Jia, J. F. Song, B. Q. Xiao, Q. Liu, H. Zhao, Z. Y. Yang, J. G. Liao, L. Y. Wu, B. Jiang, A. Atrens and F. S. Pan, *J. Mater. Res. Technol.*, 14 (2021) 1739.
6. J. L. N. Galvez-Sandoval, I. Camarillo, G. Munoz, A. N. Meza-Rocha and U. Caldino, *Opt. Mater.*, 84 (2018) 879.
7. L. Kouisni, M. Azzi, M. Zertoubi, F. Dalard and S. Maximovitch, *Surf. Coat. Technol.*, 185 (2004) 58.
8. N. R. Checca, F. F. Borghi, A. M. Rossi, A. Mello and A. L. Rossi, *Appl. Surf. Sci.*, 545 (2021) 148880.
9. W. Su, J. S. Guo, J. J. Xu, K. Huang, J. B. Chen, J. Jiang, G. M. Xie, J. Z. Zhao, S. Zhao and C. Q. Ning, *Chem. Eng. J.*, 404 (2021) 126473.
10. L. B. Zang, Y. Chen, Y. M. Wu, Y. Zheng, H. Chen, D. L. You, L. Li and J. K. Li, *Wear*, 458-459 (2020) 203427.
11. A. S. Sabau, J. Jun and D. Mcclurg, *Int. J. Adhes. Adhes.*, 102 (2020) 102641.
12. K. Cho, J. Baek, C. Balamurugan, H. Im and H. J. Kim, *J. Ind. Eng. Chem.*, 106 (2022) 537.
13. B. L. Lin, J. T. Lu and G. Kong, *Surf. Coat. Technol.*, 202 (2008) 1831.
14. K. J. Chi and Y. Huang, *J. Rare Earths*, 28 (2010) 132.
15. V. S. Saji, *J. Mater. Res. Technol.*, 8 (2019) 5012.
16. D. Ernens, M. B. D. Rooij, H. R. Pasaribu, E. J. Vanriet, W. M. Vanhaaften and D. J. Schipper, *Tribol. Int.*, 118 (2018) 474.
17. D. Weng, P. Jokiel, A. Uebleis and H. Boehni, *Surf. Coat. Technol.*, 88 (1997) 147.
18. L. Fang, L. B. Xie, J. Hu, Y. Li and W. T. Zhang, *Physics Procedia*, 18 (2011) 227.
19. R. H. Guo, J. Wang, S. L. An, J. Y. Zhang, G. Z. Zhou and L. L. Guo, *J. Rare Earths*, 38 (2020) 384.
20. M. M. Liu, H. X. Hu, Y. G. Zheng, J. Q. Wang, Z. H. Gan and S. Qiu, *Surf. Coat. Technol.*, 367 (2019) 311.
21. P. Saffarzade, A. A. Amadeh and N. Agahi, *Tribol. Int.*, 144 (2020) 106122.
22. L. F. Zhou, X. W. Gao, T. Du, H. Gong, L. Y. Liu and W. B. Luo, *J. Alloys Compd.*, 905 (2022) 163939.
23. G. W. Wang, D. Song, Y. X. Qiao, J. B. Cheng, H. Liu, J. H. Jiang, A. Ma and X. L. Ma, *J. Magnesium Alloys*, 7 (2021) 101124.
24. Z. F. Lin, W. Zhang, W. Zhang, L. K. Xu, Y. P. Xue and W. H. Li, *Mater. Chem. Phys.*, 277 (2022) 125503.
25. M. Moradi and M. Rezaei, *Constr. Build. Mater.*, 317 (2022) 126136.
26. J. P. Li, Y. M. Bian, X. H. Tu, W. Li and D. D. Song, *J. Electroanal. Chem.*, 910 (2022) 116206.
27. Y. D. Yu, Y. Cao, M. G. Li, G. Y. Wei and H. Dettinger, *Mater. Res. Innovations*, 18 (2014) 314.
28. W. L. Ma, H. X. Wang, Y. X. Wang, A. Neville and Y. Hua, *Corros. Sci.*, 195 (2022) 109947.
29. U. Sajjad, A. Abbas, A. Sadeghianjahromi, N. Abbas, J. S. Liaw and C. C. Wang, *J. Mater. Res. Technol.*, 11 (2021) 1859.
30. G. F. Chi, D. Q. Yi and H. Q. Liu, *J. Mater. Res. Technol.*, 9 (2020) 1162.
31. Z. Y. Chen, C. C. Lin, W. Zheng, Y. Zeng and Y. R. Niu, *Corros. Sci.*, 199 (2022) 110217.
32. Y. Q. Tan, W. Liao, S. Zeng, P. Jia, Z. Teng, X. S. Zhou and H. B. Zhang, *J. Alloys Compd.*, 907

(2022) 164334.
33. J. Chen, H. Y. Yang, G. Q. Xu, P. J. Zhang, J. Lv, W. Sun, B. S. Li, J. Huang, D. M. Wang, X. Shu and Y. C. Wu, *J. Rare Earths*, 40 (2022) 302.
34. Y. D. Yu, G. Y. Wei, L. Jiang and H. L. Ge, *Int. J. Electrochem. Sci.*, 15 (2020) 1108.
35. Y. C. Zou, H. Yan, B. B. Yu and Z. Hu, *Intermetallics*, 110 (2019) 106487.